MARS' UPPER ATMOSPHERE AND IONOSPHERE AT LOW, MEDIUM, AND HIGH SOLAR ACTIVITIES.

Vladimir A. Krasnopolsky , *Catholic University of America, Washington, DC, USA (vkrasn@verizonmail.com)*

Introduction:

Structure and composition of the Martian upper atmosphere and ionosphere and their response to variations of solar activity are among the important objectives to study Mars. Even the most detailed observations from the Viking entry probes are incomplete, and photochemical modeling compensates for this incompleteness and is helpful to study the processes that determine the basic properties of Mars' atmosphere and ionosphere.

The objective of this work is a self-consistent modeling of Mars' upper atmosphere and ionosphere under the specific conditions of the HST detection of D (*Krasnopolsky et al.* 1998, $F_{10.7\ cm}$= 25), the FUSE detection of H_2 (*Krasnopolsky and Feldman* 2001, $F_{10.7\ cm}$= 61), and the Mariner 6 and 7 study of Mars' hydrogen corona (*Anderson and Hord* 1971, $F_{10.7\ cm}$= 88). The models will convert the observed densities of D and H_2 to the HD and H_2 mixing ratios in the lower atmosphere, which are important for evolution of water. The model conditions correspond to low, medium, and high solar activities, respectively, and the results may be used for various applications.

Model:

The lower boundary is at 80 km because diffusion separation is negligible for all species below this height. The upper boundary is at 300 km which is close to the ionopause. The model is dayside mean (solar zenith angle = 60°). The parent species are CO_2, N_2, Ar, H_2, HD, and He. They are given at the lower boundary where $[CO_2]=2\times10^{13}$ cm^{-3} by their mixing ratios. Photochemical products are O, CO, NO, H, D and 18 ions formed by photo- and electron impact dissociation, ionization, dissociative ionization, and chemical reactions. The total number of reactions is 115 (including 29 reactions involving deuterated species).

The lower boundary conditions for photochemical products are velocities V = -K/H. (K is the eddy diffusion coefficient which also involves the mixing by large-scale winds, and H is the scale height.) The upper boundary conditions are velocities V = 0 for heavy neutral species, thermal and nonthermal escape velocities for H_2, HD, H, D, and He, and V = 3×10^4 cm/s for ions.

Nonthermal escape processes for H_2, HD, H, and D include (1) charge exchange with the solar wind protons, (2) photoionization above the ionopause, and (3) dissociation and ionization by electrons above the ionopause. Electron densities were taken from *Zhang et al.* (1993). Data on nonthermal escape of He are from *Krasnopolsky and Gladstone* (1996).

Each of our models is a solution of a set of the continuity equations for each species. The continuity equations are the second order ordinary nonlinear differential equations which involve eddy, molecular, and ambipolar diffusion and chemical sources and sinks. The equations were solved numerically with a step of 1 km. Column production and loss rates are balanced for each species within ≈1%.

Results:

The HD and H_2 mixing ratios in the lower atmosphere appeared to equal 11 ppb and 15 ppm, respectively. They have important implications for evolution of water on Mars that are not discussed here.

The results of modeling are given as vertical profiles of density for all species (Fig. 1-3) at three level of solar activity and column reaction rates. These rates may be compared to establish a relative importance of each process. Therefore the data are detailed and complete.

Two closely related values are the O/CO_2 ratio at 125 km and the O_2^+/CO_2^+ ratio at 130 km:

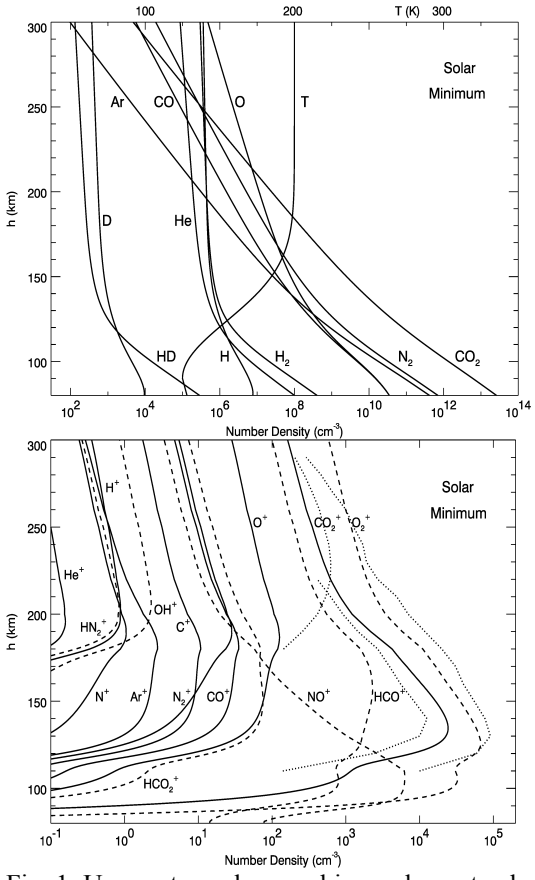

Fig. 1. Upper atmosphere and ionosphere at solar minimum. Dotted curves the Viking 1 measurements

of O^+, CO_2^+, and O_2^+ (from left to right).

$$O_2^+ / CO_2^+ = \frac{kO}{\alpha n_e}$$

($k = 2.6\times10^{-10}$ cm^{-3} s^{-1} is the rate coefficient for the reaction between CO_2^+ and O, α is the recombination coefficient for O_2^+). Then O/CO_2 = 2-3% for the Viking ionospheric data and 0.8% for the Mariner 9 observations of O 1304 Å. Evidently our models cannot fit both values, and the model results O/CO_2 = 1.3% at 125 km and $O_2^+/CO_2^+ \approx 3$ at 130 km is a reasonable compromise.

The calculated O_2^+ density profile at solar minimum agrees with the Viking measurements within a factor of 1.5-2. The difference is partly due to the different solar zenith angle (41° for the Viking measurements and 60° for the model; cos 41°/cos 60°= 1.5).

The calculated O^+ density at 180 km at solar minimum agrees with that measured by the Viking landers. However, ambipolar diffusion becomes a dominant process in my one-dimensional models and forms a peak in the O^+ distribution at 190 km, preventing a further increase in the O^+ density. The ion flow to the nightside should further diminish the O^+ densities above 190 km. I could get a better agreement with the O^+ density profile observed by the Viking entries (which has a maximum of $[O^+] \approx 600$ cm^{-3} at 225 km) by the appropriate reduction in the ambipolar diffusion coefficient for O^+. There is no physical reason, however, to do this, and I have no idea to explain the Viking profile of O^+.

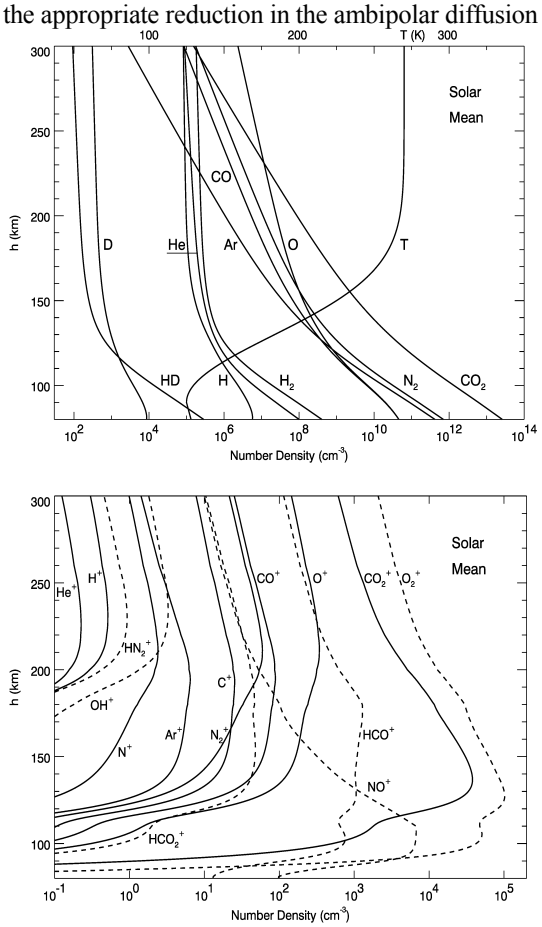

Fig. 2. Upper atmosphere and ionosphere at medium solar activity.

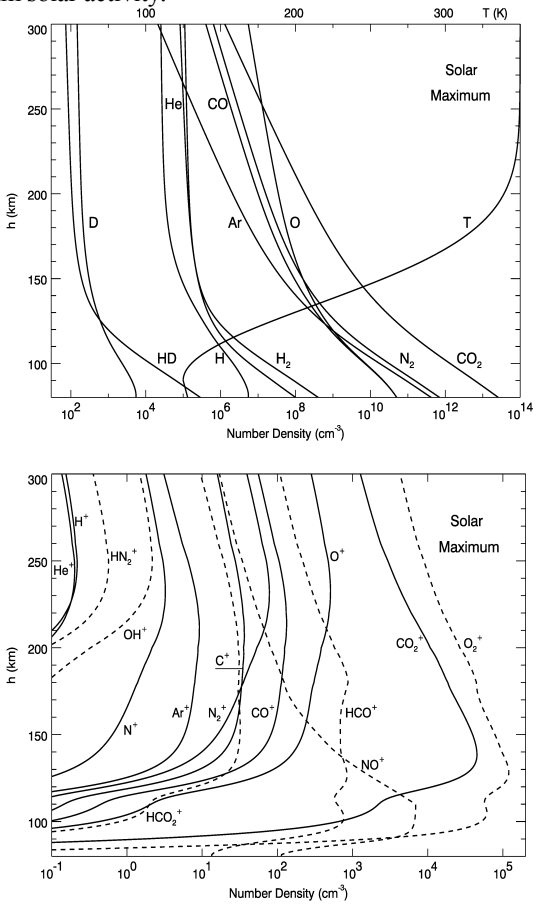

Fig. 3. Upper atmosphere and ionosphere at high solar activity.

Our models involve profiles of the hydrogen-containing ions OH^+, NH^+, HN_2^+, ArH^+, and HCO^+ that were not included in the previous models. NH^+, ArH^+, and H_2^+ densities are very low and not shown in Figure 1-3. HCO^+ does not react with the neutral species in the atmosphere and can only recombine. Therefore its densities are comparatively high, $\tilde{\approx}10^3$ cm^{-3}, especially at the low solar activity. Its mass as well as that of NO^+ is close to that of O_2^+ and may be indistinguishable for low resolution instruments as the retarding potential analyzers.

The strongest effect that affects in the ion density variations at 250-300 km is the increase of the ion and electron temperatures [*Hanson and Mantas,* 1988; *Rohrbaugh et al.,* 1979]. This increase makes the ion scale heights at 250-300 km similar and almost independent of the ion masses. There are no observational data on the variations of T_i and T_e with solar activity, therefore the same values are used in all three models. The resulting ion scale heights at 250-300 km do not vary with solar activity in my models.

The models give detailed quantitative data on each ion, its vertical profile, column production and loss

rates (Table 2), and variations with solar activity. Both the solar EUV photon flux and the thermospheric density and composition significantly vary with solar activity, and the resulting variations of ion densities are by an order of magnitude at 250-300 km and smaller at the lower heights. The number of ions is large, and I do not discuss the behavior of each species.

Acknowledgment. This work was supported by the NASA Mars Data Analysis Program under Grant NAG5-10575.

References:

Anderson, D. E., C. W. Hord, *JGR 76,* 6666, 1971

Hanson, W. B., G. P. Mantas, *JGR 93,* 7538, 1988

Krasnopolsky, V. A., P. D. Feldman, *Science 294,* 1914, 2001

Krasnopolsky, V. A., G. R. Gladstone, *JGR 101,* 15765, 1996

Krasnopolsky, V. A., M. J. Mumma, G. R. Gladstone, *Science 280,* 1576, 1998

Rohrbaugh, R. P., J. S. Nisbet, E. Bleuler, J. R. Herman, *JGR 84,* 3327, 1979

Zhang, M. H. G., J. G. Luhmann, A. F. Nagy, J. R. Spreiter, S. S. Stahara, *JGR 98,* 3311, 1993